*Desalination and Water Treatment*
www.deswater.com
doi: 10.5004/dwt.2021.27635

240 (2021) 177–190
November

# Adsorption removal of cationic dyes from aqueous solutions by raw and chemically activated cedar sawdust

Zineb Bencheqroun[a], Imane El Mrabet[a], Mostafa Nawdali[b], Mohamed Benali[c], Hicham Zaitan[a,*]

[a]*Processes, Materials and Environment Laboratory (LPME), Faculty of Sciences and Technology, Sidi Mohamed Ben Abdellah University, B.P. 2202, Fez, Morocco, emails: hicham.zaitan@usmba.ac.ma (H. Zaitan), zinebbencheqroun@yahoo.fr (Z. Bencheqroun), imane.elmrabet@usmba.ac.ma (I. El Mrabet)*
[b]*Processes, Materials and Environment Laboratory (LPME), Polydisciplinary Faculty, Sidi Mohamed Ben Abdellah University, Taza, B.P. 1223, Morocco, email: mostafa.nawdali@usmba.ac.ma*
[c]*Université de Technologie de Compiègne, ESCOM, TIMR (Integrated Transformations of Renewable Matter), Centre de Recherche Royallieu-CS 60319-60203 Compiègne, Cedex, France, email: m.benali@escom.fr*

Received 14 May 2021; Accepted 15 July 2021

**ABSTRACT**

The aim of this work is to study the removal of Basic Blue 3 (BB3) and Methylene blue (MB) from aqueous solutions using raw and chemically treated cedar sawdust as eco-friendly and sustainable bioadsorbents. The raw and treated cedar sawdust (CS) samples were activated with NaOH (0.1 N) and HCl (0.1 N) solutions. The surface characteristics of the bioadsorbents were analyzed by diverse physico-chemical methods such as scanning electron microscopy with energy-dispersive X-ray analysis, Fourier transform infrared spectroscopy, point of zero charge ($pH_{pzc}$), X-ray diffraction. The monitoring of the optimal experimental conditions of the different parameters such as dye concentration, contact time, adsorbent dose and solution pH were performed in a batch system. Experimental results show that the adsorption process is rapid and reaches equilibrium after 1 h of contact time. The adsorption capacities of the CS bioadsorbent depend on the pH of the solution and adsorbent dose. Consequently, the adsorption of BB3 and MB is favored at basic pH with the maximum adsorption percentage removal of 98% for BB3 and 99.8% for MB. Adsorption kinetics and equilibrium isotherm parameters were fit using two classic adsorption models (Langmuir and Freundlich). The adsorption kinetics of dyes onto CS followed could be described well with the pseudo-second-order model, whereas the equilibrium data fitted well to the Langmuir isotherm model with a correlating constant ($R^2$) higher than 0.98. The maximum adsorption capacities ($Q_{max}$) onto of raw-CS, HCl-CS and NaOH-CS were estimated to be 47.62, 71.94 and 76.92 mg $g^{-1}$ for MB and 33.67, 72.46 and 85.3 mg $g^{-1}$ for BB3 respectively, showing that the NaOH-CS adsorbent is about 1.6–2.6 time more efficient that the natural-CS. As a result, chemically treated cedar sawdust has great potential as an inexpensive and readily available alternative bioadsorbent for the removal of cationic dyes from industrial wastewaters.

*Keywords:* Dyes; Adsorption; Bioadsorbent; Activated cedar sawdust

* Corresponding author.

*Presented at the Second International Symposium on Nanomaterials and Membrane Science for Water, Energy and Environment (SNMS-2021), June 1–2, 2022, Tangier, Morocco*

## 1. Introduction

Wastewater effluents from the textile, food and pharmaceutical industries contain a wide variety of dyestuffs [1]. Due to their complex structure, they are very difficult to treat by conventional wastewater treatment methods (chemical or biological) [2]. In addition, the presence of synthetic dyes in natural water sources can lead to serious problems, such as risks to public health and the environment [3–5]. It is estimated that approximately 50,000 tons of dyestuffs are released annually into the effluents of the dyeing and staining industries [6]. In order to reduce all these harmful effects, it is necessary to remove dyes from industrial effluents before discharging them into the environment [7].

Many techniques have been tested and used for the treatment of effluents loaded with dyes such as membrane separation [8], ozonation [9], anodic oxidation [10,11], photocatalytic oxidation [12,13] and biological degradation [14]. However, several of these techniques have limited applicability because of the important generation of secondary pollution, high investment, operational and maintenance costs due to huge consumption of energy and chemicals [15].

Adsorption is considered an attractive method for wastewater treatment because of its low cost, simple design, ease to operate and insensitivity to toxic pollutants [16]. Activated carbon is an efficient adsorbent for wastewater treatment applications [17], but it is still considered very expensive and not able to be regenerated after use.

Therefore, the development of efficient and inexpensive alternative adsorbents for dyes removal is attracting increasing attention worldwide [10,18,19]. In this regard, raw cedar sawdust (CS) could be used as a low-cost bioadsorbent and widely available solid waste, especially after its chemical modification that has been shown to be more effective than raw sawdust in removing toxic dyes from contaminated water through an adsorption process [20] due to their relatively high specific surface areas and important concentration of functional groups that actively contribute to the fixation of dye molecules on their surface site.

Hence, the aim of this study was to contribute to the efforts of valorizing the agricultural by-products and to investigate the feasibility of applying natural and activated cedar sawdust, as an adequate bioadsorbent in the removal of two cationic dyes, Basic Blue 3 (BB3) and Methylene blue (MB) from textile industries at low cost.

The surface properties of the raw and activated chemically bioadsorbent have been characterized by several techniques, such as scanning electron microscopy (SEM) coupled with energy-dispersive X-ray analysis (EDX), Fourier transform infrared spectroscopy (FTIR), the pH of the point of zero charge ($pH_{pzc}$). In addition, the effect of different operational conditions (i.e., pH of the solution, initial dye concentration, contact time and adsorbent dosage) are evaluated. Additionally, kinetic and equilibrium models are applied to the experimental data and the best models are selected.

## 2. Materials and methods

### 2.1. Materials

The CS samples were collected from the Fez region in Morocco, and cut into small portions, then crushed using a domestic grinder. It was then washed several times with tap water, and rinsed with distilled water to remove impurities present on the surface. Samples were dried in an oven at 100°C for 24 h. Subsequently, the crushed samples were sieved through a 100 μm sieve and used in all experiments. Samples were kept in hermetic glass bottles namely as natural-CS.

Two different commercial dyes were used in this study without further purification: Basic Blue 3 (BB3) ($C_{20}H_{26}C_1N_3O$; Mw = 359.89 g $mol^{-1}$, purity > 99%, $\lambda_{max}$ = 654 nm) and Methylene blue (MB) ($C_{16}H_{18}C_1N_3S$; Mw = 319.85 g $mol^{-1}$; purity > 99%, $\lambda_{max}$ = 664 nm). They were purchased from Sigma-Aldrich Chimie S.a.r.l. (Lyon, France) and Bestchem Hungária Kft, (Budapest, Hungary), respectively.

### 2.2. Chemical treatments of cedar sawdust

In order to increase the adsorption capacity, the material underwent activation of the adsorption sites by two different chemical treatments (alkaline treatment with sodium hydroxide and an acid treatment using chloric acid).

The activation of the cedar sawdust was carried out in a 500 mL batch reactor at a temperature of 25°C. A mass of natural-CS was treated with 500 mL of 0.1 N reagent solutions (HCl (0.1 N) and/or NaOH (0.1 N)). The mixture was stirred for 24 h. The treated CS was filtered and then washed several times with distilled water until the pH was neutralized to remove the excess chemical. Finally, the recovered CS was dried at a temperature of 110°C, then crushed and sieved in a 100 μm sieve, then stored in a vacuum desiccator under to following names HCl-CS and NaOH-CS for further application.

### 2.3. Characterization of cedar sawdust

The CS bioadsorbent was subjected to physico-chemical and morphological characterization using different instrumental techniques: Brunauer–Emmett–Teller-specific surface area measurement (ASAP 2020 Micromeritics sorption analyzer, Norcross, GA, USA), X-ray diffraction (XRD, Philips Analytical X-ray PW1710 diffractometer), scanning electron microscopy (SEM, JSM-IT500HR, JEOL, Japan) and Fourier transform infrared spectroscopy (FTIR) using a VERTEX 70v spectrophotometer (Bruker Optics S.a.r.l., France) within the range of 4,000–400 $cm^{-1}$.

The pH value required to give a zero net surface charge ($pH_{pzc}$) of the CS adsorbent was determined according to the procedure described by Bencheqroun et al. [21,22].

### 2.4. Adsorption experiments

Batch adsorption experiments of dyes onto CS bioadsorbent (natural or activated) were carried out to investigate the influence of bioadsorbent dosage, pH of the solution, contact time, initial concentration dye on the dye adsorption capacity. The dose-effect of CS was studied by adding various dosages of raw or activated CS in a range of 0.02–0.6 g to flasks containing 20 mL of dye solution with concentrations ranging from 5 to 500 mg $L^{-1}$ without pH adjustment (pH = 7) at room temperature (25°C). The mixtures were

agitated at 200 rpm until reaching equilibrium using a water shaker bath for 24 h.

The adsorption kinetics were studied by introducing the optimal dose of raw CS in a volume of 500 mL of the dye without adjustment of the pH. Samples were taken after various contact times ranging from 5 to 180 min to determine the dye residual dye concentrations.

For the isotherms experiment, samples were kept in agitation for 3 h, using the optimal dose of CS (10 g $L^{-1}$ for MB and 15 g $L^{-1}$ for BB3) without adjustment of the pH (pH 7), whereas the dye concentration varied from 0 to 11,000 mg $L^{-1}$. After each experiment, the separation of the two phases (CS and dye solution) was done by centrifugation at 4000 rpm for 10 min and then the BB3 and MB residual concentrations were determined by UV-Visible spectrophotometer (UV1600 spectrophotometer) at a maximum wavelength, $\lambda_{max}$ = 654 nm for BB3, and $\lambda_{max}$ = 664 nm for MB. Dilutions were made when measurements exceeded the linearity of the calibration curves. A similar procedure was carried out for all other adsorption tests on CS. All batch experiments were performed in duplicate and the standard error was less than 4%.

The total adsorbed amount of dye at equilibrium per mass of CS ($q_e$, mg $g^{-1}$) and the adsorbed amount of dye at different time ($q_t$, mg $g^{-1}$) were determined by mass balances according to the following equation [23]:

$$q_{t,e} = \frac{\left(c_0 - c_{t,e}\right)V}{m} \quad (1)$$

The removal efficiency (%) can be calculated as follows:

$$\text{Removal}(\%) = \frac{\left(c_0 - c_{t,e}\right)}{c_0} \times 100 \quad (2)$$

where $c_0$ (mg $L^{-1}$) and $c_{t,e}$ (mg $L^{-1}$) are dye concentrations at the beginning and at specific or equilibrium time, respectively. $m$ is the mass of adsorbent (g), and $V$ is the total volume of adsorption solution (L). The influence of operating conditions on the adsorption of dye onto cedar sawdust was studied in a batch system.

## 3. Results and discussion

### 3.1. Characterisation of cedar sawdust

The specific surface area and porosity of the CS sample were determined using nitrogen adsorption–desorption at 77 K. the CS was degassed before analysis at 383 K for 4 h under vacuum at <$10^{-2}$ Pa in order to remove all physically adsorbed water molecules and small organic impurities.

The specific surface area (SBET) of CS determined using nitrogen adsorption–desorption at 77 K is presented in Fig. 1. The CS bioadsorbent has a very low specific surface area (1.33 $m^2$ $g^{-1}$). According to the IUPAC classification [24], this CS bioadsorbent is thus considered nonporous. However, this value obtained does not represent the actual pore texture available during the adsorption. Thus, the adsorption of the organic material on this material occurred according to the main mechanism that takes place in the pores or capillaries on the outer surface of the adsorbent material.

The $pH_{pzc}$ value of CS material is presented in Table 1. At pH conditions higher than the $pH_{pzc}$, the adsorbent surface will be negatively charged; which favors the adsorption of cationic dyes like BB3 and MB. Whereas, in the pH region according to the $pH_{pzc}$, positively charged sites will dominate on the adsorbent surface [25], which is in accordance with the results given by the acid-base neutralization method which justifies that acid groups are the most predominant [26].

The CS diffraction pattern has been given in Fig. 2. The peaks observed at 15° and 23° are characteristic of the

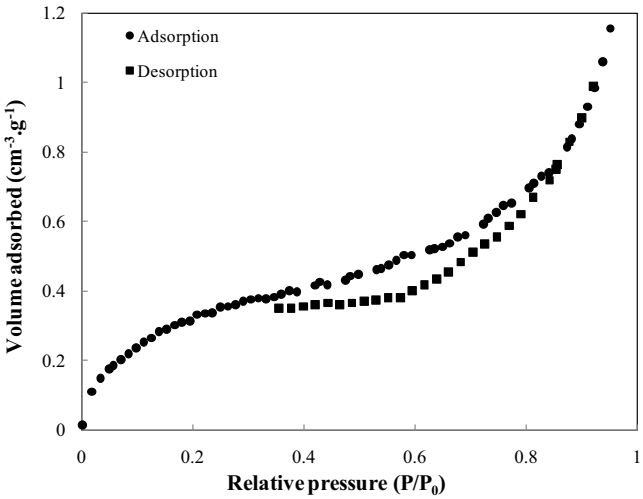


Fig. 1. $N_2$ adsorption–desorption isotherms of the CS adsorbent at 77 K: ●: adsorption;■: desorption.

Table 1
Value of $pH_{pzc}$ of natural and activated CS

| | $pH_{pzc}$ |
|---|---|
| Natural-CS | 4 |
| HCl-CS | 2.79 |
| NaOH-CS | 6.96 |

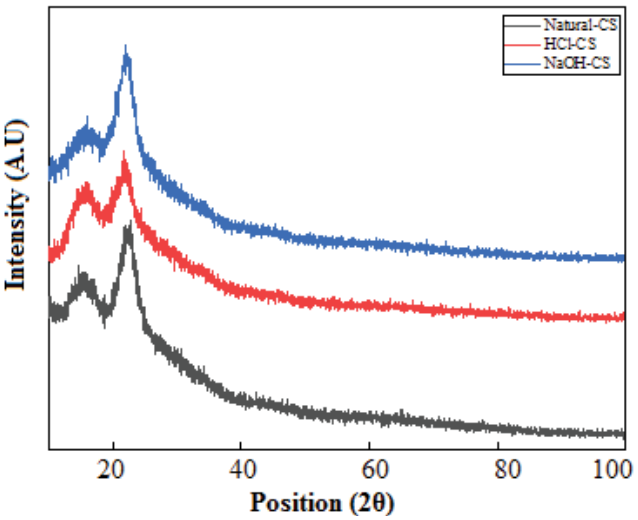


Fig. 2. X-ray patterns of natural and activated CS.

biomass of lignocellulosic CS material. The maximum peak intensity observed on 2θ of 23° corresponds to the cellulose plane (0 0 2). The lowest diffraction peak at 2θ of 15° has been attributed to lignin and hemicellulose levels, which contribute to the amorphous nature of CS [23].

The SEM-EDX technique was used in order to obtain the information on chemical composition and surface morphology of the bioadsorbent [27].

SEM images of the porosity of raw and activated cedar sawdust (natural-CS, HCl-CS and NaOH-CS) surface before adsorption are illustrates in Fig. 3. The pictures exhibit a clear sight of the pores at the surface of the bioadsorbents. The raw CS surface morphology appeared to possess an uneven structure and porous cavities. With these characteristics, the CS surface morphology can be considered very adequate as an active site for the adsorption of dyes. Similarly, the pictures show a significant difference between the surface morphology of the raw and treated CS. From Fig. 3 it can be seen that NaOH is an effective agent in creating well-developed pores on the surface of the CS bioadsorbent. The chemically activated sawdust shows a well-developed surface morphology that is clearly visible with the existence of a heterogeneous porous structure that provides a large surface area that allows easy access for bioadsorption of the dyes.

The results of quantitative content of CS bioadsorbent obtained by EDX method [28] are given in Table 2.

The main components of CS are carbon (61.02%) and oxygen (38.98%). The CS is lignocellulosic biomass mainly composed of cellulose, hemicellulose and lignin, which contribute to the distribution of various oxygen functional groups on the biosorbent surface.

The FTIR analysis was used in the paper to identify the characteristic functional groups present on the surface of CS bioadsorbents and responsible for the removal of dyes from the aqueous solutions.

The FTIR spectrum of raw and treated CS (Fig. 4) revealed the presence of a broad and strong absorption band around 3,500–3,200 $cm^{-1}$ with an intense band at approximately 3,350 $cm^{-1}$ which may be attributed to the overlapping of O–H and C–H stretching vibration in hemicelluloses, cellulose and lignin. This band is characteristic of the stretching vibration of hydrogen bonding of the hydroxyl group linked in cellulose, lignin, adsorbed water, and N–H Stretching. The band at 2,925 $cm^{-1}$ is attributed to the asymmetric or symmetric C–H stretching vibrations of cellulose and hemicelluloses aliphatic [29].

The absorption peak observed at 1,630 $cm^{-1}$ is assigned to stretching vibration of carboxyl groups of the acetyl, or

Table 2
Quantitative composition of CS adsorbent dye EDX analysis

| Element | Weight (%) |
|---|---|
| C | 61.02 |
| O | 38.98 |
| Total | 100.00 |

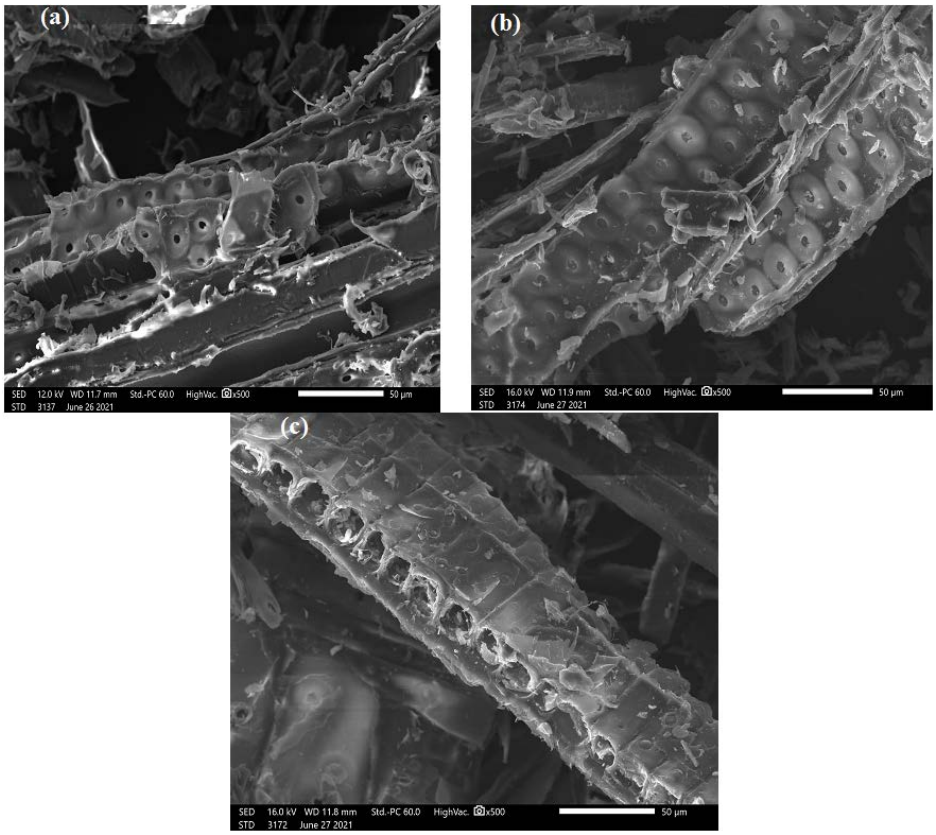


Fig. 3. SEM images of CS: (a) natural-CS, (b) HCl-CS and (c) NaOH-CS (1,000×).

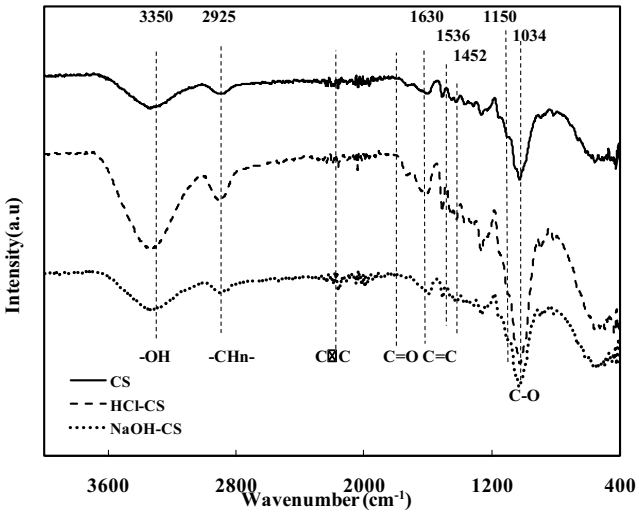


Fig. 4. FTIR spectrum of the raw and activated CS.

uronic ester groups of hemicelluloses [30]. The peaks registered in the range of 1,250 and 1,536 $cm^{-1}$ could be ascribed to a conjugated hydrogen-bonded carbonyl group. The peak at 1,452 $cm^{-1}$ indicated the presence of the functional groups C–O–H, C–O and C–H related to carboxylic acids groups [31]. The band at 893 $cm^{-1}$ is related to C–H rocking vibrations of cellulose. The C–C ring breathing band at 1,150 $cm^{-1}$ can be attributed to the presence of cellulose in the CS structure.

It is to highlight that the complete disappearance of the absorption band at 1,735 $cm^{-1}$ disappeared after the alkaline treatment of CS by NaOH. This band is typical of the carbonyl functions of carboxylic acids, esters and aldehyde groups related to lignin.

Consequently, the FTIR results indicated that the bioadsorbents presented different functional groups (hydroxyl, carboxyl and carbonyl), which may be potential bioadsorption sites for BB3 and MB dyes.

### 3.2. Effect of the bioadsorbent dose

The influence of the raw and activated CS dosage on dye removal and adsorbed amount of dye at 25°C and pH 7 was investigated by varying the bioadsorbent dose from 0.025–0.6 g using 20 mL of the 300 mg $L^{-1}$ solutions of BB3 and MB (Fig. 5).

As seen from Fig. 5, increasing the CS dosage from 0.025 to 0.2 g for BB3 and 0.3 for MB leads to the greatest dye reduction from 39% to 92% for MB and 57% to 99% for BB3 which is due to the high availability of adsorption sites. The high dye removal efficiency measured for the optimum dose of CS (0.2 g of CS for MB and 0.3 g CS for BB3) are 92% and 99%, respectively. Increasing the bioadsorbent dosage beyond this mass of CS, the dye removal efficiency changed a little. This behavior may be due to the number of adsorption sites that increases with the amount of adsorbent up to the optimal masses at which the number of sites becomes stable. This behavior can be explained by: As long as the amount of adsorbent added to the dye solution is low, the cations of the dye can easily access the adsorption sites. The addition of adsorbent increases the number of adsorption sites, but the dye cations have more difficulty approaching molecules to adsorption sites on the CS bioadsorbent due to the bulkiness. A large amount of adsorbent creates agglomerations of the bioadsorbent particles, resulting in a reduction in the total adsorption surface area and, consequently, a decrease in the amount of adsorbate per unit mass of adsorbent.

It can also be observed that the adsorption capacity of raw and activated CS towards MB and BB3 decreases with the increase of the adsorbent dose, which may be due to particle interaction (aggregation).

Therefore, the experimental results showed that the optimal dosage of CS bioadsorbent was established at 10 g $L^{-1}$ for BB3 and 15 g $L^{-1}$ for MB. This is the optimal dose of CS bioadsorbent to be applied in subsequent tests.

### 3.3. Effect of solution pH

The pH of the aqueous solution is an important process control parameter in the dye adsorption process. The effect of pH was studied at different pH values (2–12) employing the dye concentration of 300 mg $L^{-1}$ with an adsorbent dose of 10 g $L^{-1}$ for BB3 and 15 g $L^{-1}$ for MB at a temperature of 298 K for 3 h contact time.

The effect of solution pH on the removal efficiency of MB and BB3 by the raw and activated cedar sawdust is shown in Fig. 6. It is clear that the bioadsorption of the two dyes was low in an acidic medium and increases with increasing the solution pH. The removal efficiency of the two dyes (MB and BB3) by NaOH-CS reached 98% for BB3 and 99.8% for MB, followed by the activated HCl-CS and the natural-CS. It is noticed that the removal efficiency of the two dyes was gradually increased with increasing pH from 2 to 8, then it became stable after pH 8. This may be due to the fact that the carboxyl and hydroxyl active sites of the biosorbents get deprotonated and the surface of the sawdust is negatively charged at pH > $pH_{pzc}$, which favors the adsorption of the cationic dyes BB3 and MB onto the bioadsorbent. On the other hand, at pH values < $pH_{pzc}$, the surface of the sawdust is positively charged, and therefore capable of repelling the cations of the dye. As pH decreases, the number of negatively charged sites decreases, and the number of positively charged sites increases [32,33].

### 3.4. Adsorption kinetics

In order to assess the influence of contact time on the adsorption of MB and BB3 from aqueous solutions by the raw, HCl-CS and NaOH-CS, a kinetic study was performed for contact time varying from 1 to 180 min. The results of the experiments are represented in Fig. 7.

The adsorption was found to be rapid during the initial period (0–20 min) of the bioadsorption process due to the presence of a large number of sites of adsorption on CS bioadsorbent accessible for dyes molecules. Then, the rate of adsorption gradually becomes slower and it stagnates corresponding to the equilibrium point. With increasing bioadsorption time, there was a decrease in the amount of easily accessible surface adsorption sites for the residual dye molecules interaction. The equilibrium time was 1 h for both dyes (BB3 and MB) onto natural and activated CS.

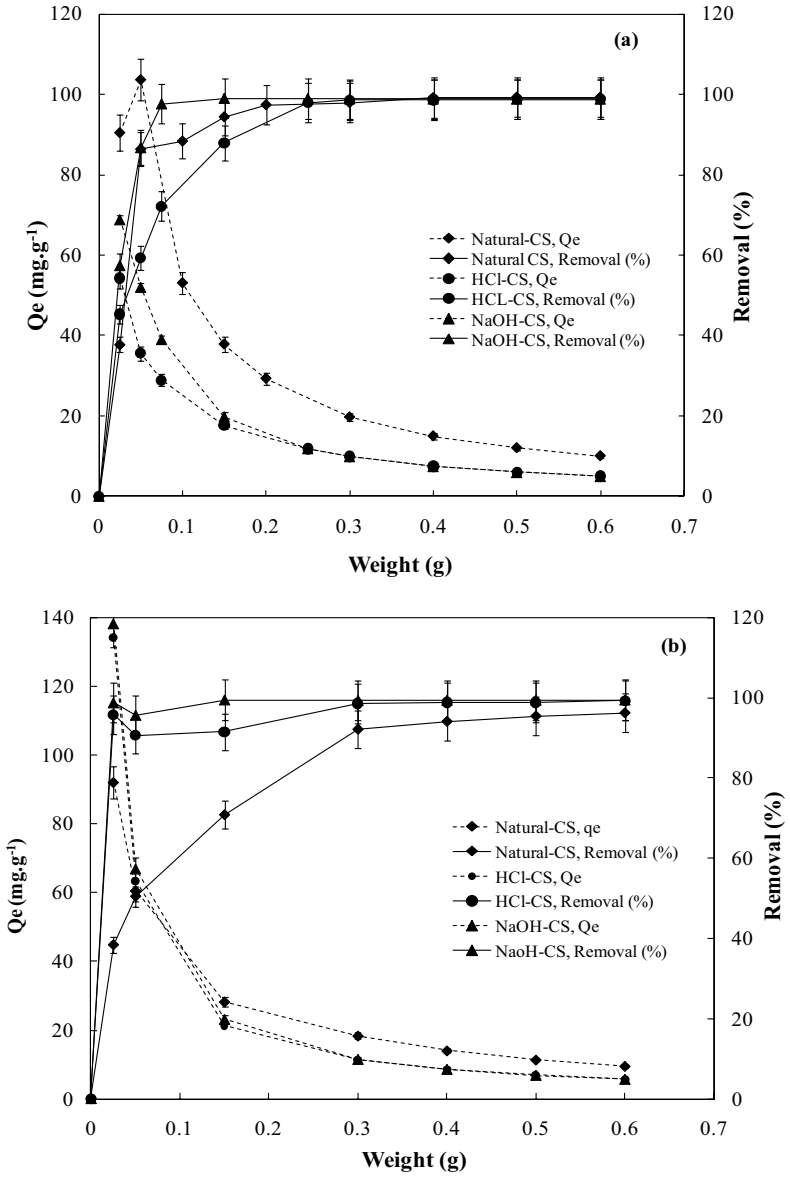


Fig. 5. Effect of the mass on the adsorption of BB3 and MB onto raw and activated CS: (a) BB3 and (b) MB. Experimental conditions: initial concentration: 300 mg $L^{-1}$; contact time = 3 h; agitation speed = 200 rpm; $T$ = 25°C.

In order to characterize the kinetics involved in the adsorption process, the experimental data were analyzed using two different kinetic models like pseudo-first-order and pseudo-second-order. Where the kinetic data were analyzed based on the regression coefficient ($R^2$) and the adsorbed amount of dye. The pseudo-first-order kinetic model [34] is given according to the following equation:

$$q_t = q_e\left(1 - e^{-k_1 t}\right) \tag{3}$$

where $q_t$ and $q_e$ are the adsorption capacity at time $t$ and equilibrium time, respectively and $k_1$ is the pseudo-first-order model rate constant. The pseudo-second-order kinetic model [35–37] is represented in Eq. (4):

$$q_t = \frac{k_2 q_e^2 t}{1 + k_2 q_e t} \tag{4}$$

where $k_2$ (g $mg^{-1}$ $min^{-1}$) is the adsorption rate constants for the pseudo-second-order kinetic model.

The correlation coefficients $R^2$ nearest to ~1 confirm that the best fit of the adsorption data of the two dyes (BB3 and MB) onto the three bioadsorbents (natural CS, HCl-CS and NaOH-CS) are given by the pseudo-second-order kinetic model as shown in Table 3. Furthermore, the values of the adsorption capacity $Q_{max}$ calculated by the pseudo-second-order model agree well with the experimental values $q_{exp}$ when compared with the values given by the pseudo-first-order model. These results suggest that

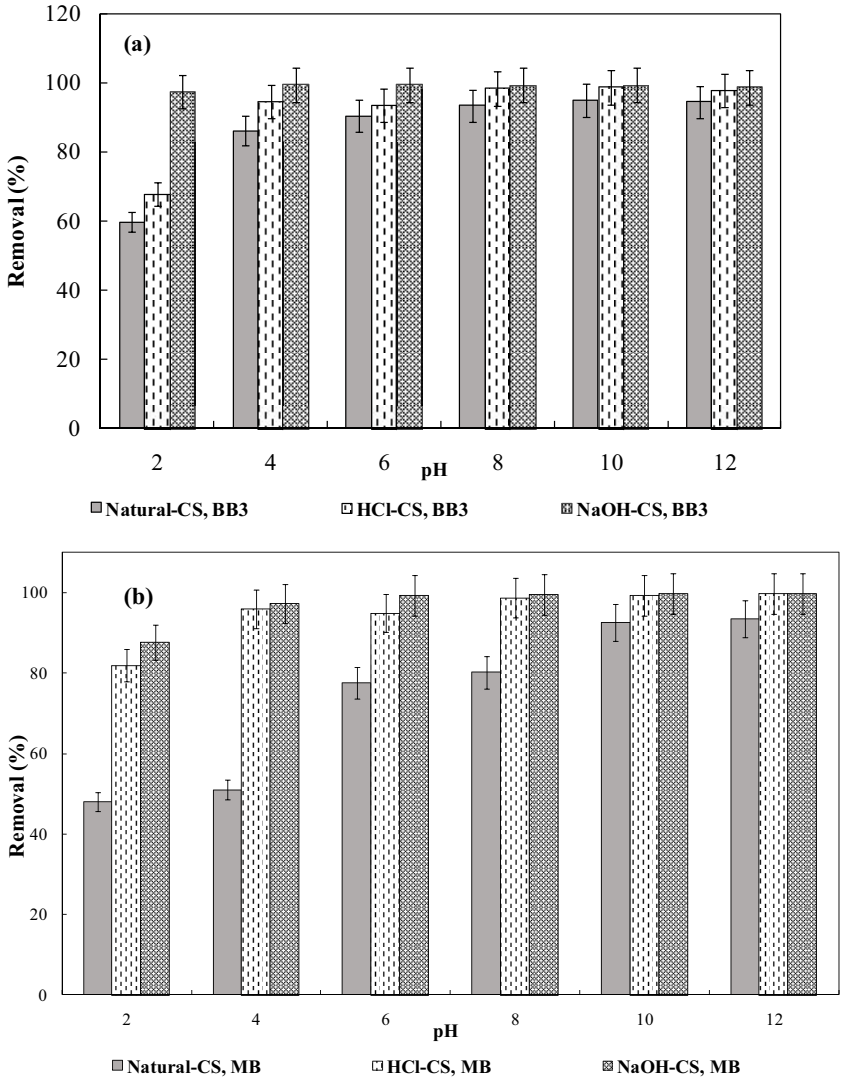


Fig. 6. Effect of the pH on the adsorption of (a) BB3 and (b) MB onto natural-CS, HCl-CS and NaOH-CS. Experimental conditions: initial concentration: 300 mg $L^{-1}$; contact time = 3 h; weight ratio = 10 g $L^{-1}$ for BB3 and 15 g $L^{-1}$ for MB; agitation speed = 200 rpm; $T$ = 25°C.

chemical interactions are responsible for the adsorption of BB3 and MB by natural and activated CS by the establishment of electronic bonding between the functional groups on the surface of the CS and the molecule of MB or BB3, which involves electrostatic interactions, hydrogen-bonding formation, electron donor-acceptor or π–π dispersion interaction [38].

### 3.5. Adsorption isotherms

The adsorption capacity of the natural and activated cedar sawdust for BB3 and MB was assessed on the basis of adsorption isotherms. Fig. 8 represents the total adsorbed amount of dyes onto raw and treated cedar sawdust bioadsorbent at the equilibrium ($q_e$).

In order to understand the nature of the interaction between CS and dyes, two isotherm models like Langmuir and Freundlich [39,40] were applied in the present study.

The mathematical expressions for these models are presented in Eqs. (5) and (6), respectively.

$$q_e = \frac{q_m K_L C_e}{1 + K_L C_e} \tag{5}$$

$$q_e = K_F C_e^{1/n} \tag{6}$$

where $K_L$ (L $mg^{-1}$) is the Langmuir equilibrium constant related to the energy of adsorption. $q_m$ and $q_e$ (mg $g^{-1}$) are the maximum and the equilibrium adsorption capacities of the Langmuir model, respectively. $C_e$ (mg $L^{-1}$) is the equilibrium concentration of the adsorbate. $K_F$ (L $mg^{-1}$) is the Freundlich constant and 1/$n$ is the heterogeneity factor.

Based on the obtained results in Fig. 8, it is noted that the adsorbed amount increases with increasing equilibrium concentration. This augmentation was due to a high driving force for mass transfer at high concentration in solution indicating that cedar sawdust has a high affinity for BB3 and MB. In fact, high concentration in solution implicates high dye fixed at the surface of the biodsorbents. The isotherms form was type L for raw-CS and HCl-CS and NaOH-CS.

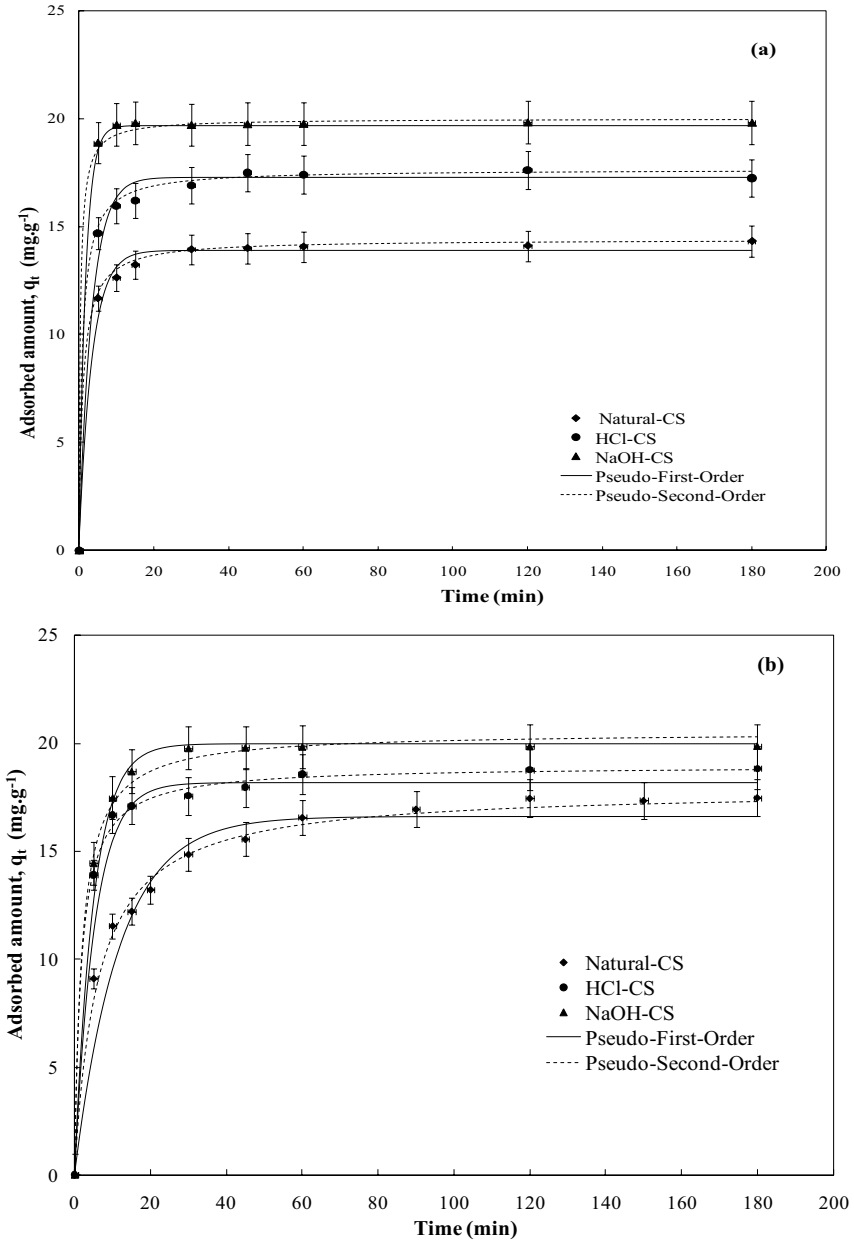


Fig. 7. Effect of contact time on the adsorption of (a) BB3 and (b) MB onto CS. Experimental conditions: initial concentration: 300 mg $L^{-1}$; contact time = 3 h; weight ratio = 10 g $L^{-1}$ for BB3 and 15 g $L^{-1}$ for MB; agitation speed = 200 rpm; $T$ = 25°C.

Table 3
Kinetic model parameters of BB3 and MB dyes adsorption onto CS

| | | Pseudo-first-order | | | Pseudo-second-order | | |
|---|---|---|---|---|---|---|---|
| | | $Q_{max}$ | $k_1$ | $R^2$ | $Q_{max}$ | $k_2$ | $R^2$ |
| BB3 | Natural-CS | 13.91 | 0.29 | 0.91 | 14.39 | 0.06 | 0.99 |
| | HCl-CS | 17.29 | 0.29 | 0.91 | 17.64 | 0.06 | 0.98 |
| | NaOH-CS | 19.69 | 0.55 | 0.95 | 20.00 | 0.13 | 0.97 |
| MB | Natural-CS | 16.60 | 0.09 | 0.94 | 17.92 | 0.009 | 0.96 |
| | HCl-CS | 18.20 | 0.19 | 0.95 | 18.98 | 0.03 | 0.97 |
| | NaOH-CS | 20.00 | 0.20 | 0.91 | 20.55 | 0.03 | 0.98 |

The maximum Langmuir monolayer biosorption capacities ($Q_{max}$) were estimated to 47.62, 71.94 and 76.92 mg $g^{-1}$ for MB and 33.67, 72.46 and 85.3 mg $g^{-1}$ for BB3 respectively, in the case of Raw-CS, HCl-CS and NaOH-CS, showing that the NaOH-CS adsorbent is about 1.6–2.6 time more efficient that the natural-CS.

The adsorption performance of BB3 and MB by CS changes according to different criteria such as molecular weight, molecule size, chemical charge and structure, and adsorbent properties. The reason for the better adsorption of BB3 and MB is the highest negative charge present on the surface of cedar sawdust, which has been justified, by net surface charge ($pH_{pzc}$) and acid-base neutralization method and the surface charge of the dyestuffs, which is positive.

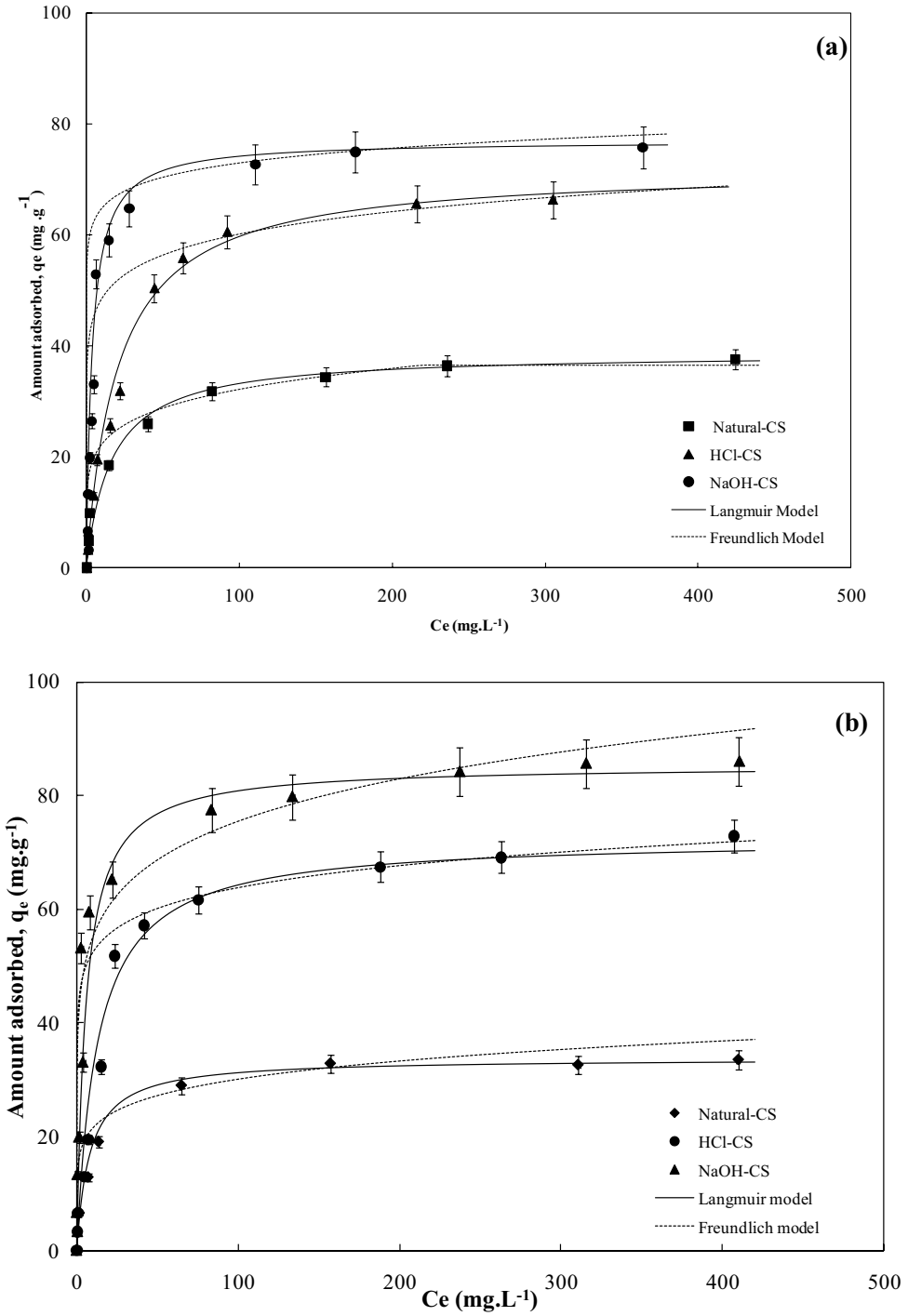


Fig. 8. Equilibrium data of (a) BB3 and (b) MB adsorption onto CS. Experimental conditions: contact time = 3 h; weight ratio = 10 g $L^{-1}$ for BB3 and 15 g $L^{-1}$ for MB; agitation speed = 200 rpm; $T$ = 25°C.

From these results, it can be noted that MB dye has a higher affinity for superficial functional groups in comparison with BB3. Also, it can be concluded that NaOH-CS adsorption capacity is better than that of raw-CS and HCl-CS due to the effect of the CS treatment since NaOH molecules affect the constructive of CS, rearrange the lignin and hemicelluloses matrix fibers, created well developed pores on the surface of the CS and lead to the appearance of negatively charged sites on the cellulose chains and new functional groups. These newly generated functional groups could present favorable linking sites for the MB and BB3 dyes adsorption and consequently enhances the removal of these kinds of dyes from aqueous solutions [38].

The adjustment of the experimental data is given by the non-linear regression method (Table 4), which is based on the regression coefficient $R^2$ of the two isothermal models

(Langmuir and Freundlich). The Langmuir model is the most suitable to characterize the adsorption isotherm with a high regression coefficient of $R^2 = 0.98$.

A comparison between the maximum bioadsorption capacities of CS for the removal of dyestuffs and other bioadsorbent was presented in Table 5. The CS showed a relatively better bioadsorption potential for the removal of BB3 and MB. The availability and cost-effectiveness of CS will provide a low-cost source of bioadsorbent for the sequestration of toxic dyes in industrial effluents.

### 3.6. Proposed mechanism for MB and BB3 adsorption onto CS

The adsorption mechanisms can be elucidated based on the analyses of raw and treated CS before and after adsorption of MB and BB3 by FTIR and SEM analysis. The results of CS characterization showed that it has a material composed of celluloses, hemicelluloses and lignins. The chemical heterogeneity of the bioadsorbent surface with irregular and different sizes and shapes was confirmed by the SEM and FTIR analysis. The components of CS bioadsorbent were rich in hydroxyls, carbonyls, ethers, phenols, aldehydes, and aromatic compounds.

Electrostatic attractions can occur between the negatively charged sites on the surface of CS and the cationic MB and BB3 molecules in the solution ($R–N^+$). The pH of the solution used in this study was ~7 and at this pH value, the (–COOH) groups of CS are ionized, forming negatively charged carboxylate (–COO–) groups. At this pH, the dispersed positive charge in MB ($R–N^+$) is expected to have a weak electrostatic interaction with the ($C–O^-$) and (COO–) sites in the adsorbent (Fig. 9).

The interactions can occur between the surface hydrogens of the hydroxyl groups on the CS surface and the nitrogen, oxygen atoms and H-acceptors of MB and BB3 and between the hydroxyl groups on the CS surface and the benzene rings of two dyes MB and BB3.

The FTIR results demonstrated that the –OH groups at 3,350 $cm^{-1}$ shifted toward slightly higher wavenumbers (Fig. 10), confirming the existence of both dipole–dipole. The carbonyl oxygens on the surface of the adsorbent act as electron donors, and the aromatic rings of MB and BB3 act as electron acceptors. After adsorption of MB and BB3, some bands were shifted (1,630 $cm^{-1}$) due to the adsorption of MB and BB3 on the surface of the CS bioadsorbent [47]. The adsorption of MB and BB3 onto CS adsorbent would take place include Van der Waals interactions and π-π stacking interaction between the benzene rings of two dyes and the delocalized-electron system of the bioadsorbent.

SEM images of CS bioadsorbents (raw CS, HCl-CS and NaOH-CS) after MB and BB3 adsorption provide additional information about the adsorption mechanisms.

Fig. 11 illustrates the porosity of the bioadsorbents surface through SEM images of raw CS and NaOH-CS surface before and after adsorption of MB and BB3. Fig. 11a and j exhibit a clear sight of the pores at the surface of the adsorbent with an irregular structure, rough and porous surface. The CS bioadsorbents surface morphology appeared to possess an uneven structure and porous cavities. However, its surface morphology changed considerably by MB and BB3 adsorption and the surface of raw CS and NaOH-CS was thoroughly covered by two dyes molecules MB and/or BB3 dye via the adsorption process onto CS and NaOH-CS, as shown in Fig. 11c, e, i, k.

The EDX analysis of raw CS and NaOH-CS revealed the presence of C, O or Na (Fig. 11b and h) but after MB and BB3 adsorption, one new peak of S element has appeared which also indicated the adsorption of MB or BB3 on the surface of CS (Fig. 11d, f, j, l).

Table 4
Isotherm constant parameters and correlation coefficients calculated for BB3 and MB adsorption onto raw CS

| | | Langmuir model | | | Freundlich model | | |
|---|---|---|---|---|---|---|---|
| | | $Q_{max}$ | $K_L$ | $R^2$ | $1/n$ | $K_F$ | $R^2$ |
| BB3 | Natural-CS | 47.62 | 0.01 | 0.98 | 0.34 | 4.96 | 0.81 |
| | HCl-CS | 71.94 | 0.05 | 0.98 | 0.009 | 38.9 | 0.88 |
| | NaOH-CS | 76.92 | 0.26 | 0.98 | 0.05 | 57.45 | 0.92 |
| MB | Natural-CS | 33.67 | 0.12 | 0.98 | 0.15 | 15.48 | 0.97 |
| | HCl-CS | 72.46 | 0.08 | 0.98 | 0.08 | 43.07 | 0.94 |
| | NaOH-CS | 85.3 | 0.18 | 0.98 | 0.14 | 40.37 | 0.82 |

## 4. Conclusion

Adsorbents prepared from cedar sawdust were successfully used to remove cationic dyes Basic Blue 3 and

Table 5
Comparison of biosorption capacities of CS with different bioadsorbents for the removal of BB3 and MB

| Bioadsorbent | Bioadsorption capacities (mg $g^{-1}$) | | References |
|---|---|---|---|
| | MB | BB3 | |
| Raw CS | 33.67 | 47.62 | Present study |
| *Posidonia oceanica* | 5.56 | – | [41] |
| Cashew nut shell | 5.31 | – | [42] |
| Coconut coir dust | 29.50 | – | [43] |
| *Azadirachta indica* leaf powder | 19.61 | – | [44] |
| Durian peel | – | 49.50 | [45] |
| *Macroalgae Caulerpa lentillifera* | – | 49.26 | [46] |

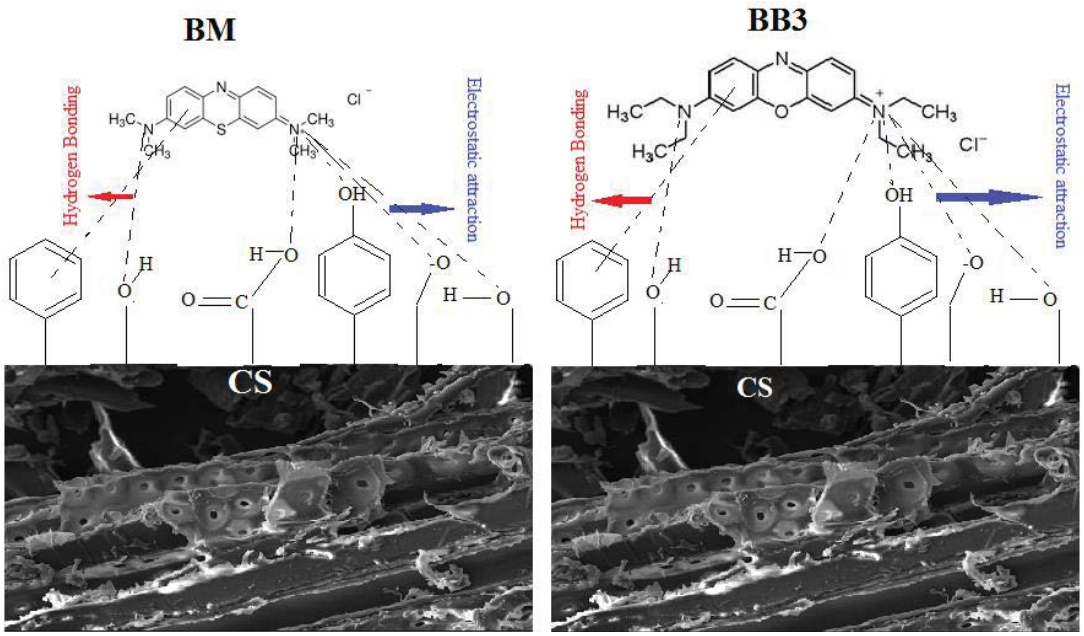


Fig. 9. Proposed mechanism of MB and BB3 adsorption on CS bioadsorbent.

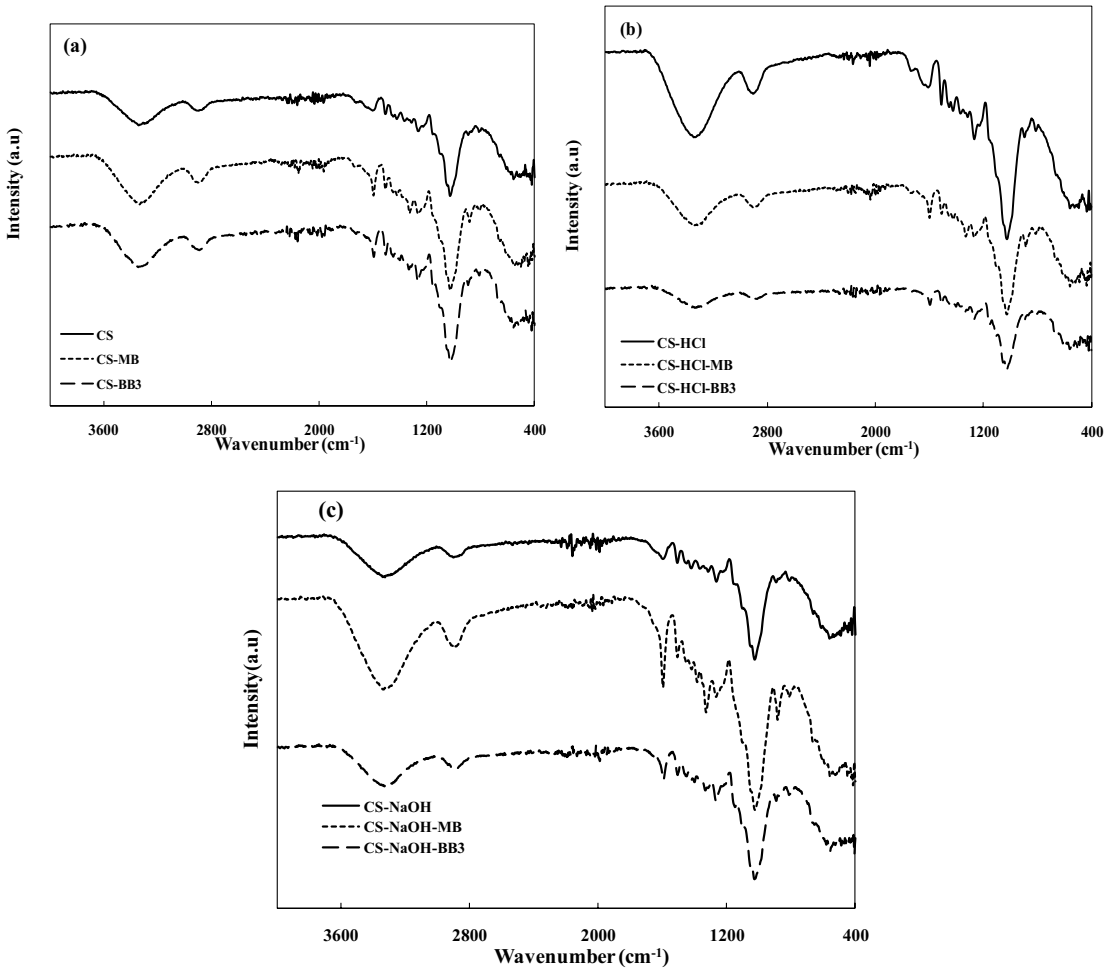


Fig. 10. FTIR spectra of the biosorbents before and after MB and BB3 adsorption, (a) natural-CS, (b) HCl-CS and (c) NaOH-CS.

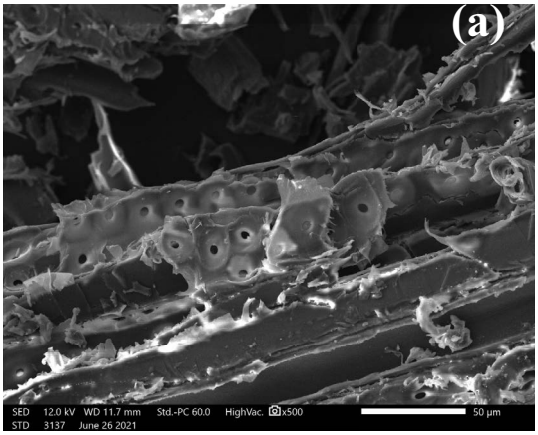
(a)
SED 12.0 kV WD 11.7 mm Std.-PC 60.0 HighVac. x500 50 µm
STD 3137 June 26 2021

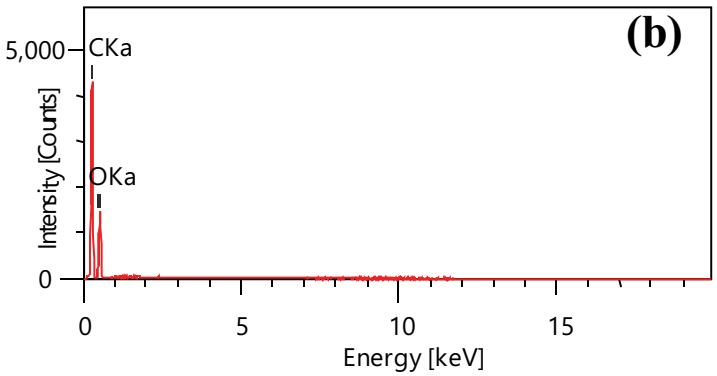
(b)
5,000
CKa
OKa
Intensity [Counts]
0
0
5
10
15
Energy [keV]

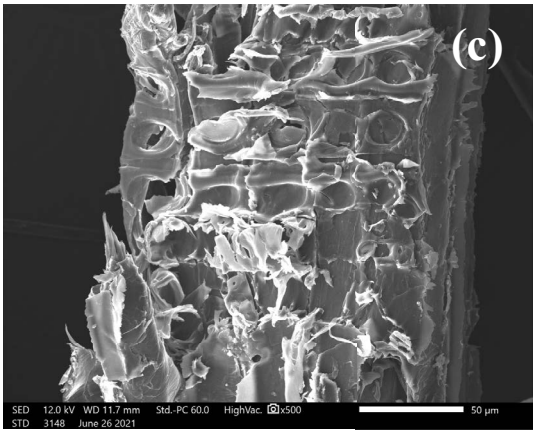
(c)
SED 12.0 kV WD 11.7 mm Std.-PC 60.0 HighVac. x500 50 µm
STD 3148 June 26 2021

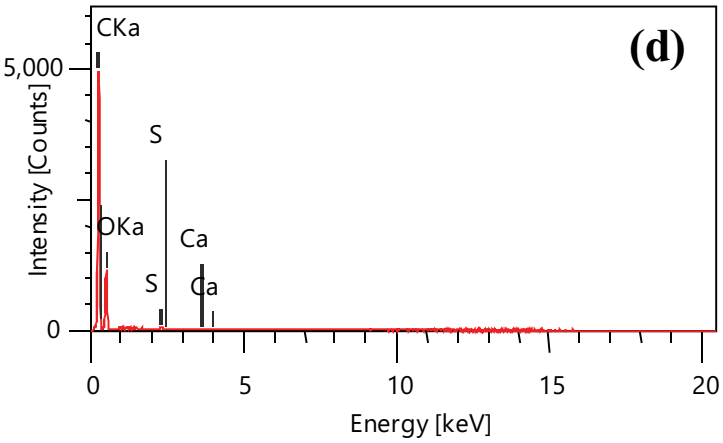
(d)
5,000
CKa
S
OKa
Ca
S
Ca
Intensity [Counts]
0
0
5
10
15
20
Energy [keV]

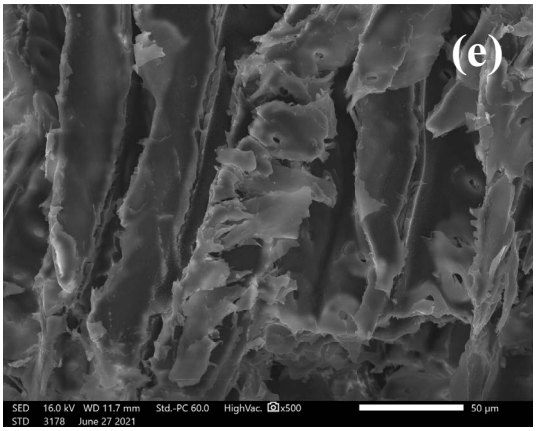
(e)
SED 16.0 kV WD 11.7 mm Std.-PC 60.0 HighVac. x500 50 µm
STD 3178 June 27 2021

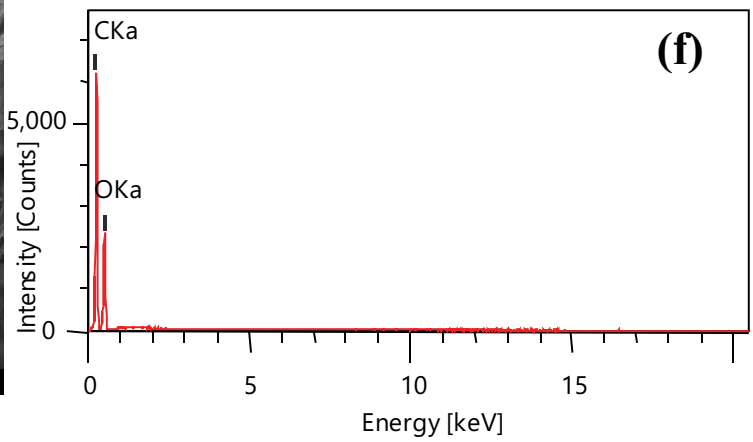
(f)
5,000
CKa
OKa
Intensity [Counts]
0
0
5
10
15
Energy [keV]

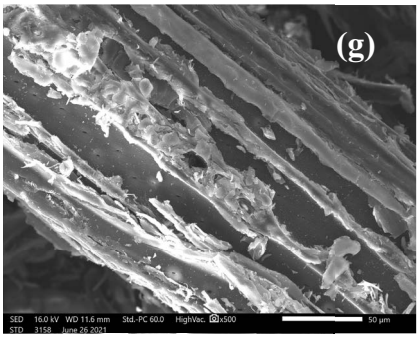
(g)
SED 16.0 kV WD 11.6 mm Std.-PC 60.0 HighVac. x500 50 µm
STD 3158 June 26 2021

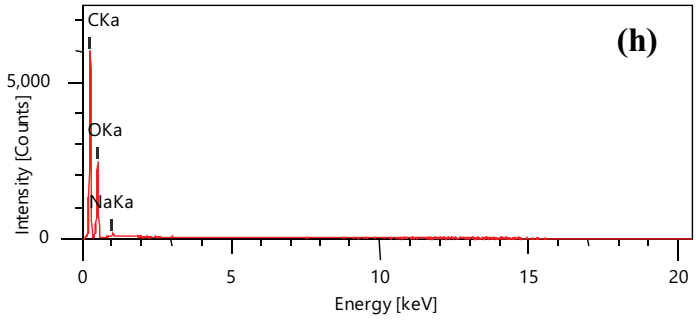
(h)
5,000
CKa
OKa
NaKa
Intensity [Counts]
0
0
5
10
15
20
Energy [keV]

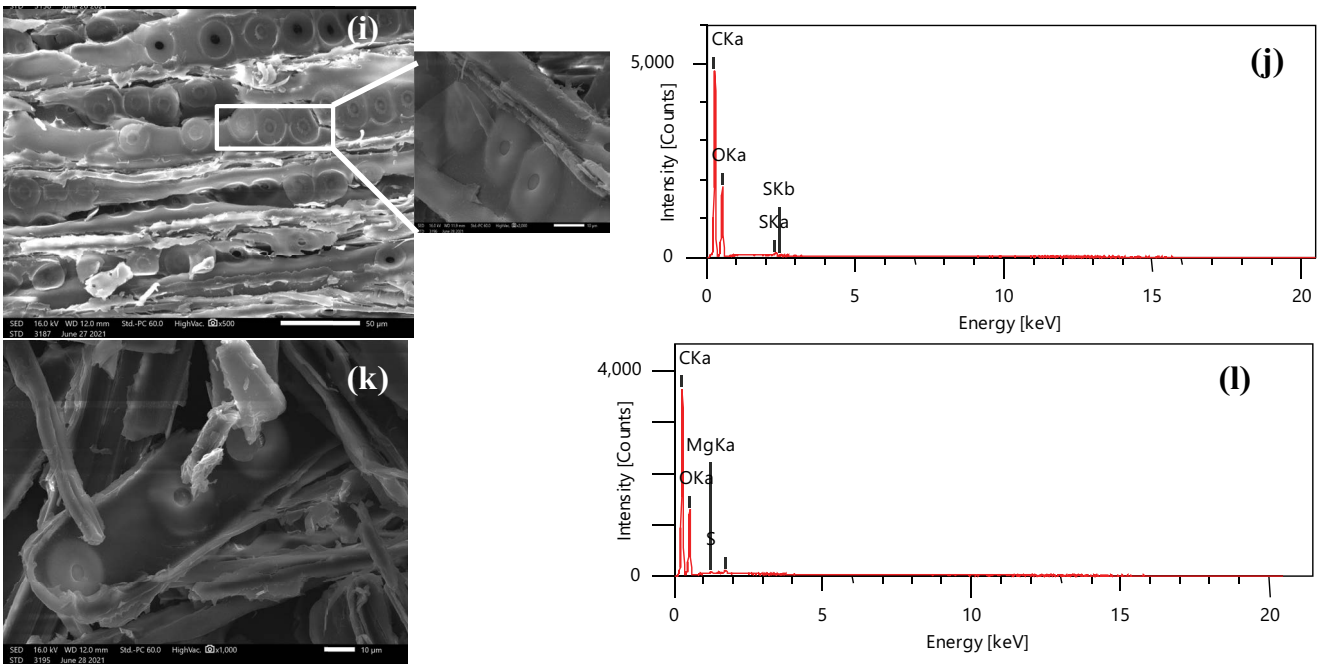


Fig. 11. SEM images for raw CS and CS-NaOH before and after adsorption of MB and BB3: (a) raw CS, (c) CS-MB, (e) CS-BB3, (g) CS-NaOH, (i) CS-NaOH-MB, (k) CS-NaOH-BB3 and EDX analysis before and after adsorption of MB and BB3 (b), raw CS, (d) CS-MB, (f) CS-BB3, (h) CS-NaOH, (j) CS-NaOH-MB, and (l) CS-NaOH-BB3.

Methylene blue from an aqueous solution. The results obtained for BB3 and MB indicate that the activated cedar sawdust exhibited a higher percentage removal (94% for both BB3 and MB dyes) when evaluating the effects of initial concentration, contact time and pH in aqueous solutions compared to that of raw cedar sawdust, which showed lower values for BB3 and MB. Natural and activated cedar sawdust can remove cationic dyes better in dye mixtures. The adsorption kinetics of BB3 and MB on activated and row sawdust was best described using a pseudo-second-order model, indicating that the adsorption mechanism of BB3 and MB on adsorbents is governed by chemisorption. The mechanism of the adsorption process was determined based on an intraparticle diffusion model. The adsorption data was well described by a model Langmuir isotherm. It is concluded that the activated sawdust prepared from cedar sawdust can be used as a natural and abundant resource for the removal of Basic Blue 3 and Methylene blue from wastewater.

## Funding sources

No funding was allowed to this work.

## References

[1] S.J. Allen, G. Mckay, J.F. Porter, Adsorption isotherm models for basic dye adsorption by peat in single and binary component systems, J. Colloid Interface Sci., 280 (2004) 322–333.
[2] S. Khaoulani, H. Chaker, C. Cadet, E. Bychkov, L. Cherif, A. Bengueddach, S. Fourmentin, Wastewater treatment by cyclodextrin polymers and noble metal/mesoporous $TiO_2$ photocatalysts, C.R. Chim., 18 (2015) 23–31.
[3] S. Bentahar, A. Dbik, M. El Khomri, N. El Messaoudi, A. Lacherai, Adsorption of Methylene blue, crystal violet and congo red from binary and ternary systems with natural clay: kinetic, isotherm, and thermodynamic, J. Environ. Chem. Eng., 5 (2017) 5921–5932.
[4] Y. Cheng, H. Lin, Z. Chen, M. Megharaj, R. Naidu, Biodegradation of crystal violet using Burkholderia vietnamiensis C09V immobilized on PVA-sodium alginate-kaolin gel beads, Ecotoxicol. Environ. Saf., 83 (2012) 108–114.
[5] V.K. Garg, M. Amita, R. Kumar, R. Gupta, Basic dye (Methylene blue) removal from simulated wastewater by adsorption using Indian Rosewood sawdust: a timber industry waste, Dyes Pigm., 63 (2004) 243–250.
[6] E. Pajootan, M. Arami, N.M. Mahmoodi, Binary system dye removal by electrocoagulation from synthetic and real colored wastewaters, J. Taiwan Inst. Chem. Eng., 43 (2012) 282–290.
[7] A. Ausavasukhi, C. Kampoosaen, O. Kengnok, Adsorption characteristics of Congo red on carbonized leonardite, J. Cleaner Prod., 134 (2016) 506–514.
[8] M. Soniya, G. Muthuraman, Recovery of Methylene blue from aqueous solution by liquid–liquid extraction, Desal. Water Treat., 53 (2013) 2501–2509.
[9] A.K.H. Al Jibouri, J. Wu, S.R. Upreti, Continuous ozonation of Methylene blue in water, J. Water Process Eng., 8 (2015) 142–150.
[10] A.A. Azzaz, S. Jellali, H. Akrout, A.A. Assadi, L. Bousselmi, Dynamic investigations on cationic dye desorption from chemically modified lignocellulosic material using a low-cost eluent: dye recovery and anodic oxidation efficiencies of the desorbed solutions, J. Cleaner Prod., 201 (2018) 28–38.
[11] H. Akrout, S. Jellali, L. Bousselmi, Enhancement of Methylene blue removal by anodic oxidation using BDD electrode combined with adsorption onto sawdust, C.R. Chim., 18 (2015) 110–120.
[12] A.A. Azzaz, A.A. Assadi, S. Jellali, A. Bouzaza, D. Wolbert, S. Rtimi, L. Bousselmi, Discoloration of simulated textile effluent in continuous photoreactor using immobilized titanium dioxide: effect of zinc and sodium chloride, J. Photochem. Photobiol., A, 358 (2018) 111–120.
[13] G. Sharma, A. Kumar, S. Sharma, Mu. Naushad, P. Dhiman, D.-V.N. Vo, F.J. Stadler, $Fe_3O_4$/ZnO/$Si_3N_4$ nanocomposite based photocatalyst for the degradation of dyes from aqueous

solution, Mater. Lett., 278 (2020) 128359, doi: 10.1016/j.matlet.2020.128359.
[14] F. Ding, Y. Xie, W. Peng, Y.K. Peng, Measuring the bioactivity and molecular conformation of typically globular proteins with phenothiazine-derived Methylene blue in solid and in solution: a comparative study using photochemistry and computational chemistry, J. Photochem. Photobiol., B, 158 (2016) 69–80.
[15] S. Jellali, E. Diamantopoulos, K. Haddad, M. Anane, W. Durner, A. Mlayah, Lead removal from aqueous solutions by raw sawdust and magnesium pretreated biochar: experimental investigations and numerical modelling, J. Environ. Manage., 180 (2016) 439–449.
[16] N.K. Amin, Removal of reactive dye from aqueous solutions by adsorption onto activated carbons prepared from sugarcane bagasse pith, Desalination, 223 (2008) 152–161.
[17] W. Li, Q. Yue, P. Tu, Z. Ma, B. Gao, J. Li, X. Xu, Adsorption characteristics of dyes in columns of activated carbon prepared from paper mill sewage sludge, Chem. Eng. J., 178 (2011) 197–203.
[18] M.M. Hassan, C.M. Carr, A critical review on recent advancements of the removal of reactive dyes from dyehouse effluent by ion-exchange adsorbents, Chemosphere, 209 (2018) 201–219.
[19] A.B. Albadarin, M.N. Collins, M. Naushad, S. Shirazian, G. Walker, C. Mangwandi, Activated lignin-chitosan extruded blends for efficient adsorption of Methylene blue, Chem. Eng. J., 307 (2017) 264–272.
[20] R. Djeribi, O. Hamdaoui, Sorption of copper(II) from aqueous solutions by cedar sawdust and crushed brick, Desalination, 225 (2008) 95–112.
[21] Z. Bencheqroun, I. El Mrabet, M. Kachabi, M. Nawdali, H. Valdés, I. Neves, H. Zaitan, Removal of basic and acid dyes from aqueous solutions using cone powder from Moroccan cypress *Cupressus sempervirens* as a natural adsorbent, Desal. Water Treat., 166 (2019) 387–398.
[22] Z. Bencheqroun, I. El Mrabet, M. Kachabi, M. Nawdali, I. Neves, H. Zaitan, Removal of basic dyes from aqueous solutions by adsorption onto Moroccan Clay (Fez City), Mediterr. J. Chem., 8 (2019) 158, doi: 10.13171/mjc8319050803hz.
[23] M. Bhaumik, R. McCrindle, A. Maity, Efficient removal of Congo red from aqueous solutions by adsorption onto interconnected polypyrrole-polyaniline nanofibres, Chem. Eng. J., 228 (2013) 506–515.
[24] D. Everett, Manual of symbols and terminology for physicochemical quantities and units, Appendix II: definitions, terminology and symbols in colloid and surface chemistry, Pure Appl. Chem., 31 (1972) 577–638.
[25] J.P. Reymond, F. Kolenda, Estimation of the point of zero charge of simple and mixed oxides by mass titration, Powder Technol., 103 (1999) 30–36.
[26] H.P. Boehm, Some aspects of the surface chemistry of carbon blacks and other carbons, Carbon, 32 (1994) 759–769.
[27] Y. Okuyama, K. Matsumoto, H. Okochi, M. Igawa, Adsorption of air pollutants on the grain surface of Japanese cedar pollen, Atmos. Environ., 41 (2007) 253–260.
[28] A.K. Jain, V.K. Gupta, A. Bhatnagar, Suhas, Utilization of industrial waste products as adsorbents for the removal of dyes, J. Hazard. Mater., 101 (2003) 31–42.
[29] Y. Dai, Q. Sun, W. Wang, L. Lu, M. Liu, J. Li, S. Yang, Y. Sun, K. Zhang, J. Xu, W. Zheng, Z. Hu, Y. Yang, Y. Gao, Y. Chen, X. Zhang, F. Gao, Y. Zhang, Utilizations of agricultural waste as adsorbent for the removal of contaminants: a review, Chemosphere, 211 (2018) 235–253.
[30] L. Borah, M. Goswami, P. Phukan, Adsorption of Methylene blue and eosin yellow using porous carbon prepared from tea waste: adsorption equilibrium, kinetics and thermodynamics study, J. Environ. Chem. Eng., 3 (2015) 1018–1028.
[31] A. Xu, L. Cao, B. Wang, Facile cellulose dissolution without heating in $[C_4mim][CH_3COO]$/DMF solvent, Carbohydr. Polym., 125 (2015) 249–254.
[32] S.S. Tahir, N. Rauf, Removal of a cationic dye from aqueous solutions by adsorption onto bentonite clay, Chemosphere, 63 (2006) 1842–1848.
[33] C.H. Weng, Y.F. Pan, Adsorption of a cationic dye (Methylene blue) onto spent activated clay, J. Hazard. Mater., 144 (2007) 355–362.
[34] A. Gupta, C. Balomajumder, Simultaneous adsorption of Cr(VI) and phenol onto tea waste biomass from binary mixture: multicomponent adsorption, thermodynamic and kinetic study, J. Environ. Chem. Eng., 3 (2015) 785–796.
[35] X. Guo, J. Wang, A general kinetic model for adsorption: theoretical analysis and modeling, J. Mol. Liq., 288 (2019) 111100, doi: 10.1016/j.molliq.2019.111100.
[36] M. Hadri, Z. Chaouki, K. Draoui, M. Nawdali, A. Barhoun, H. Valdés, N. Drouiche, H. Zaitan, Adsorption of a cationic dye from aqueous solution using low-cost moroccan diatomite: adsorption equilibrium, kinetic and thermodynamic studies, Desal. Water Treat., 75 (2017) 213–224.
[37] Z.R. Yet, M.Z.A. Rahim, Removal of methyl red from aqueous solution by adsorption on treated banana pseudostem fibers using response surface method (RSM), Malaysian J. Anal. Sci., 18 (2014) 592–603.
[38] A.A. Azzaz, S. Jellali, A.A. Assadi, L. Bousselmi, Chemical treatment of orange tree sawdust for a cationic dye enhancement removal from aqueous solutions: kinetic, equilibrium and thermodynamic studies, Desal. Water Treat., 3994 (2015) 1–13.
[39] I. Langmuir, The adsorption of gases on plane surfaces of glass, mica and platinum, J. Am. Chem. Soc., 40 (1918) 1361–1403.
[40] A. Mittal, L. Kurup, J. Mittal, Freundlich and Langmuir adsorption isotherms and kinetics for the removal of Tartrazine from aqueous solutions using hen feathers, J. Hazard. Mater., 146 (2007) 243–248.
[41] M.C. Ncibi, A.M.B. Hamissa, A. Fathallah, M.H. Kortas, T. Baklouti, B. Mahjoub, M. Seffen, Biosorptive uptake of Methylene blue using Mediterranean green alga *Enteromorpha* spp., J. Hazard. Mater., 170 (2009) 1050–1055.
[42] P. Senthil Kumar, R.V. Abhinaya, K. Gayathri Lashmi, V. Arthi, R. Pavithra, V. Sathyaselvabala, S. Dinesh Kirupha, S. Sivanesan, Adsorption of Methylene blue dye from aqueous solution by agricultural waste: Equilibrium, thermodynamics, kinetics, mechanism and process design, Colloid J., 73 (2011) 651–661.
[43] U.J. Etim, S.A. Umoren, U.M. Eduok, Coconut coir dust as a low cost adsorbent for the removal of cationic dye from aqueous solution, J. Saudi Chem. Soc., 20 (2016) S67–S76.
[44] K.G. Bhattacharya, A. Sharma, Kinetics and thermodynamics of Methylene blue adsorption on Neem (*Azadirachta indica*) leaf powder, Dyes Pigm., 65 (2005) 51–59.
[45] S.T. Ong, S.Y. Tan, E.C. Khoo, S.L. Lee, S.T. Ha, Equilibrium studies for Basic Blue 3 adsorption onto durian peel (*Durio zibethinus Murray*), Desal. Water Treat., 45 (2012) 161–169.
[46] P. Waranusantigul, P. Pokethitiyook, M. Kruatrachue, E.S. Upatham, Kinetics of basic dye (Methylene blue) biosorption by giant duckweed (*Spirodela polyrrhiza*), Environ. Pollut., 125 (2003) 385–392.
[47] H.N. Tran, S.-J. You, H.-P. Chao, Fast and efficient adsorption of methylene green 5 on activated carbon prepared from new chemical activation method, J. Environ. Manage., 188 (2017) 322–336.